

# The Application of Cretaceous Clay Minerals of Mjez El Beb (North-Western Tunisia) in Ceramic Industry

Hammami-Ben Zaid Faten<sup>1\*</sup>, Sghaier Dalel<sup>1</sup>, Slim-Shimi Najet<sup>1</sup> and Henchiri Mohsen<sup>2</sup>

<sup>1</sup>Department of Geology, Faculty of Sciences of Tunis University Campus 2092, El Manar, Tunisia

<sup>2</sup>Department of Geology, Faculty of Sciences of Gafsa, Sidi Ahmed Zarrouk, Gafsa 2112, Tunisia

## Abstract

The Cretaceous clays of north-western Tunisia have been studied for their use in the traditional ceramic industry (bricks, tiles and pottery). Mineralogical, chemical, thermal analyses, technological proprieties and grain size distribution were carried out on clay samples collected from Jebel El Moura (BM section) and kef Lasfar-Oued El Jebbs (MK section) in the locality of Mjez el Beb. The results showed that these clay minerals are represented mainly by kaolinite associated with illite and smectite. Quartz, calcite, feldspars and hematite were also detected as accessory minerals in the whole rock. The amount silica is convenient for the manufacture of ceramic products. So the prepared mixtures were made without admixture of any variety of silicate. The technology tests revealed that the modelled products had small shrinkage during drying and firing, and a high bending strength. For this reason, the clay mixtures were made without admixture of quartz or any other component. As a result, Mjez el Beb clays have high qualities necessary for the manufacture of tiles and ceramic bricks.

**Keywords:** Ceramic industry; Clays; Cretaceous; Jebel el Moura; North-western of Tunisia; Technology tests

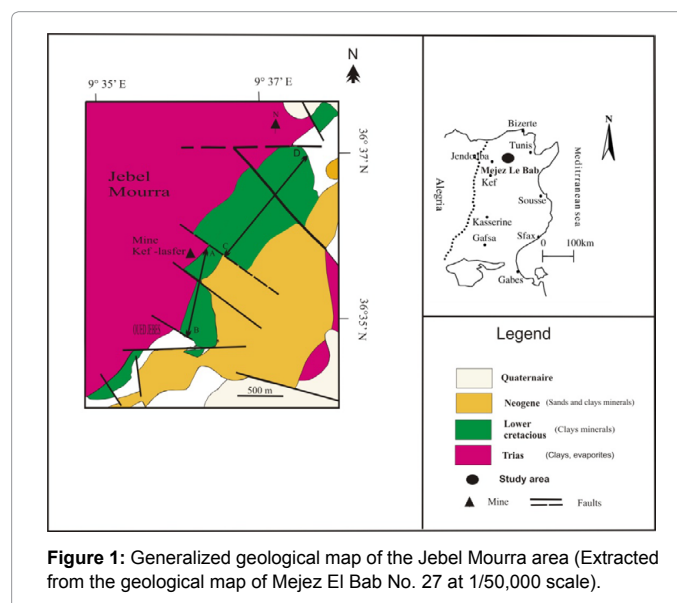
## Introduction

Clay minerals likely have a great range of applications, including agriculture (soils that grow plants), oil absorbents, iron casting, animal feeds, pharmaceuticals, drilling fluids, waste water treatment, paint, paper, paint, petroleum industry, cat litter, catalysis, ceramic etc., Their applications are tightly dependent upon their structure, composition, and physical properties [1]. Knowing these characteristics may help to better use in many fields especially in the ceramic industry. In particular, kaolinite and illite are the preferred type of clay for the traditional ceramic industry, since they can be easily moulded, and have a fine g and a moderate plasticity. Besides, they are the purest clays, since they have a low Cation Exchange Capacity (CEC), and therefore very little in composition. Moreover, they do not absorb water and do not expand when they come in contact with water that makes them ideal for industrial applications. These non-swelling clays are widely exposed in many areas, especially in north Tunisia, where a large occurrence of cretaceous clays have been reported in Jebel Mourra (Mjez El Beb, Tunisia) [2]. This raw material is the subject of this research which deals with the physico-chemical properties of two clay mixtures of Mjez el Beb (BM and MK sections) in order to assess the possibility of using them in faience and brick productions (Figure 1).

## Geological Setting

The study area is located at 8 Km in the south Mjez El Beb city (in the northern Tunisia). It consists of a NE-SW-trending anticline-like structure. Previous studies [3-7] showed that the Triassic gypsiferous cap rock constitutes the core of this structure bounded on its south-eastern flank by Cretaceous and Tertiary sediments. These later are cut by NW-SE and SE-NW to E-W faults. This structure is the result of an extensive tectonic regime affecting the north of Tunisia during the Cretaceous resulting from the convergence of African and Eurasian plates. From a paleogeographic perspective, this area belongs to the "Sillon Tunisien" (an E-W to SW-NE Tunisian Trough), which results from the Tethyan rifting events [3]. The Early Cretaceous to Early Albian marls and clayey limestones were separated from Late Albian to Paleocene shales and limestones by a regional unconformity [8,9].

Two N-S-trending geological sections, are located in the SE flank of Jebel Mourra, and consist of Cretaceous clay formations (Figure 2). Regarding, El Mourra outcrops (BM section), a 1700 m thick clayey series of beige and gray to brownish colour containing few beds of fine limestone with beige, and grey patina in breakage (Figure 2a). The series



**\*Corresponding author:** Hammami-Ben Zaid Faten, Department of Geology, Faculty of Sciences of Tunis University Campus 2092, El Manar, Tunisia, Tel : 0021626308661; E-mail: [faten0hammami@yahoo.fr](mailto:faten0hammami@yahoo.fr)

Received September 07, 2015; Accepted October 06, 2015; Published October 16, 2015

**Citation:** Faten HBZ, Dalel S, Najet SS, Mohsen H (2015) The Application of Cretaceous Clay Minerals of Mjez El Beb (North-Western Tunisia) in Ceramic Industry. J Earth Sci Clim Change. 6: 308. doi:10.4172/2157-7617.1000308

**Copyright:** © 2015 Faten HBZ, et al. This is an open-access article distributed under the terms of the Creative Commons Attribution License, which permits unrestricted use, distribution, and reproduction in any medium, provided the original author and source are credited.

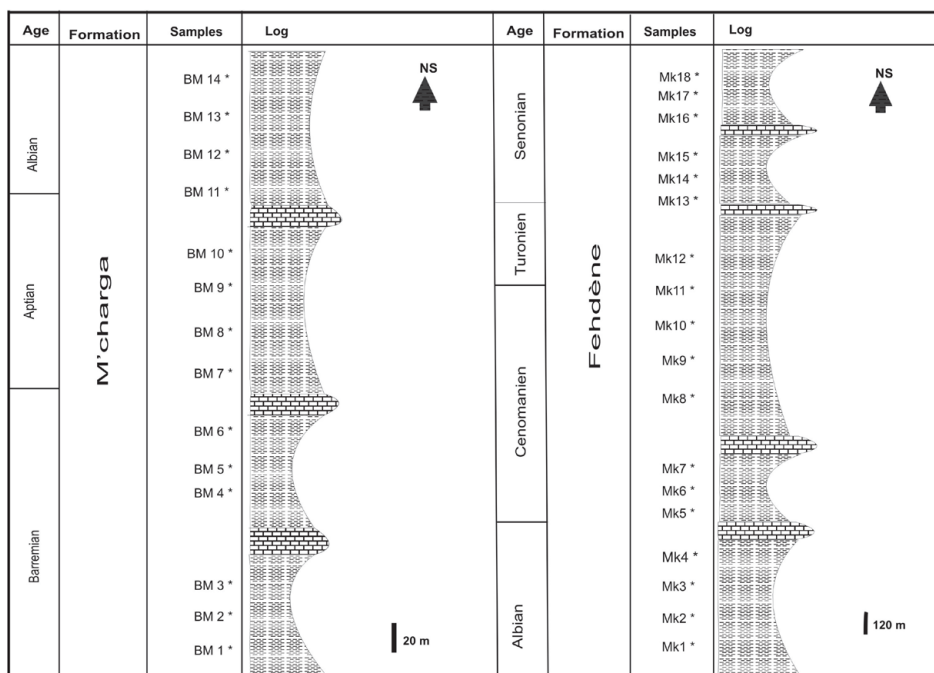


Figure 2: Synthetic lithostratigraphic log of Mourre (a) and Kef Lasfer-OuedJebbes (b) sections.

dates to the Early Cretaceous witnessed by the following fauna species: *Lenticulina Ouacheniss*, *Epistomina (Brotzena) djaffaensis* [10,11], *Globuligerina hoterivica* [10-12], *Hedbergella tuschepsensis*, *Leupoldina pustulans*, *Biglobigernella barri*. The lithological series of Kef Lasfer-Oued Jebes (MK section) includes five clay combs varying from beige, greenish to grey in colour, and with a thickness ranging from 150 to 480 m (Figure 2b). Faunistic species namely: *Thalmaninella appenninica ballernaensis* were found in these tender levels, which let us to attribute these series from Albian to Senonian age. These argillaceous combs contain metre-scale alternations of beige pelagic limestone units.

## Materials and Methods

More than 50 Kg of raw materials were collected from this Mjez el Beb clay deposits. Eighteen samples were taken from kef Lasfer-Oued El Jebes section and fourteen specimens were sampled from jebel El Mourra section. One representative mixture for the whole lower Cretaceous clays (BM section) and another one (MK section) of the Upper Cretaceous clay have been considered to define the potential use of these raw materials in the ceramic industry. Therefore, BM and MK clays were used in the ceramic earthen ware, while BM and MK samples were mixed to make up the bricks. The bulk material was initially dried at 60°C for 24 h, and then was gently crushed. Mineralogical analysis was carried out by X-ray diffraction (XRD) using a PANalytical X'Pert Pro diffractometer, operating at 40 kV and 40 mA; and equipped with a Cu K $\alpha$  radiation (1.5418 Å). The relative abundances of non-clay species was estimated using the heights ratio of the main reflections whereas, clay minerals proportions were determined by measuring the superficies of the "001" reflections. Infrared spectra were obtained using a JASCO FT-IR-420 spectrophotometer. The pressed-discs, we prepared using 1 mg of the selected samples which was diluted with 200 mg KBr. Discs were heated on the oven overnight at 150°C to minimize the water absorption on KBr and the clay powder. Transmittance spectra were recorded in the MIR region 4000 to 400 cm<sup>-1</sup>. The cation exchange capacity was measured with standard acetate ammonium procedure.

Chemical compositions of powdered and pressed clays samples were determined by subjecting them to an electron microprobe equipped with an X-ray dispersive spectrometer (Bruker S4 Pioneer). Samples preparation was realized according to the conventional techniques proposed by Meseguer et al. [13]. The particle-size distribution was obtained by laser granulometry using a MALVERN instrument. Thermal Gravimetric Analysis (TGA) and Differential Thermal Analysis (DTA) were performed with a SETRAM type 124 TG/DTA instrument using aluminium as inert reference material. Temperature was increased from room temperature to 1100°C at the regular increment of 10°C/min in air atmosphere. The expansion and firing shrinkage were measured using the dilatometer Adamel Lhomargy Type DM 15. The powders were heated from room temperature above 1200°C with 10°C/min. The liquid limit (LL), plastic limit (PL) and plastic index (IP), (IP=LL-PL) were determined for each sample in accordance with the French Standard NF P 94-051. The Bigot curve drawn with an Adamel barelattograph is used to characterize the drying process. The ceramic properties, namely moisture content dry shrinkage and dry bending strength were performed on fired products. The linear firing shrinkage, the bending strength and the water absorption for ceramic faience, were obtained from modelling numerous flat pieces (with normative dimensions: 100 mm×50 mm×10 mm). After compacting of 60 g moistened materials (7wt.% moisture content) under 250 bars, the prepared pieces were oven-dried at 105°C until constant weight then fired at 950°C and at 1000°C during 1h. The water absorption for ceramic faience was determined by immersing a specimen of brick in water boiling until constant mass. The water absorption by dipping (Abs) is expressed as a percentage of the dry weight and is calculated by the following relationship: Abs = 100 x (mh - ms)/ms. mh, constant wet mass of the specimen after immersion; ms, constant dry mass of the specimen wiped with an absorbing any water surface rag. The bending strength was measured with a three point flexural method according to the norm [14]. The linear firing shrinkage, the bending strength and the water absorption were carried out for ceramic bricks pieces heated in

three stage of temperature: 800°C, 850°C, 900°C, at heating rate 5 °C/min and the soaking time 1 hour.

## Results and Interpretations

### Mineralogy characterization

**Particle size:** The grading curves of (BM) and (MK) mixtures have a bimodal distribution: a dominant particle-size population having diameters ranging between approximately 30 µm and 25 µm; a second population with diameters lower than 4 µm (Table 1 and Figure 3). The D50 and D90 particle-size represent the median diameters which range between 8.97 µm and 39.47 µm for BM, and 15.77 µm and 48.02 µm for MK. This later is related to the presence of the kaolinite. The fraction below 2 µm corresponds to 40.38% and 38.7% of the whole sample for MK and BM respectively. These values are suitable for the ceramic manufacture.

**X-ray Diffraction:** The results summarized in Table 2 show the predominance of kaolinite (48% for BM and 41% for MK), and

Mixtures	D <sub>10</sub>	D <sub>50</sub>	D <sub>90</sub>
BM	1.50	8.97	39.47
MK	2.33	15.77	48.02

Table 1: Particle size distribution.

smectite (46% for BM and 38% for MK) and low to moderate content of illite (20% for MK and 6% for BM). The mineralogical analysis of the non-clay minerals indicates the presence of quartz (51% in the MK samples and 35% in the BM samples), calcite and the feldspars which the content not exceeds the 6%, and, the hematite which is only detected in the MK sample (2%).

**Infrared spectroscopy:** The IR absorption curves of both clay samples BM and MK are roughly similar, as seen in (Figures 4 and 5). It shows the presence of OH-stretching bands at the vicinity of 3600-3700 cm<sup>-1</sup> domain and the Si-O stretching bands near 1000 cm<sup>-1</sup> [15-19]. Bands at 3698 cm<sup>-1</sup>, and 3620 cm<sup>-1</sup> are attributed to the structural OH respectively of kaolinite [15,16,20,21]. The broad OH-stretching band ranging from 3623 and 3926 cm<sup>-1</sup> coupled with relatively weak absorption bands near 825 and 750 cm<sup>-1</sup> are characteristic of illite. The latter bands arise from Al-Mg-OH deformation. The shoulder at 913 cm<sup>-1</sup> is attributed to the Al-OH-Al bending vibration and characterise the dioctahedral phyllosilicates [22]. The peak at 885 cm<sup>-1</sup> is assigned to the Fe-Al-OH vibration that identified usually in the illite and smectitic minerals [23] resulting from Fe<sup>3+</sup> for Al substitution in the octahedral sheet. The shoulder arising from the Si-O-Al vibration is showed at 536 cm<sup>-1</sup>. The presence of water is verified by the band large at 3400 cm<sup>-1</sup>. Peaks at 1727, 1402, 875 and 712 cm<sup>-1</sup> correspond to the presence of calcite. The quartz was identified in the two samples by the bands at

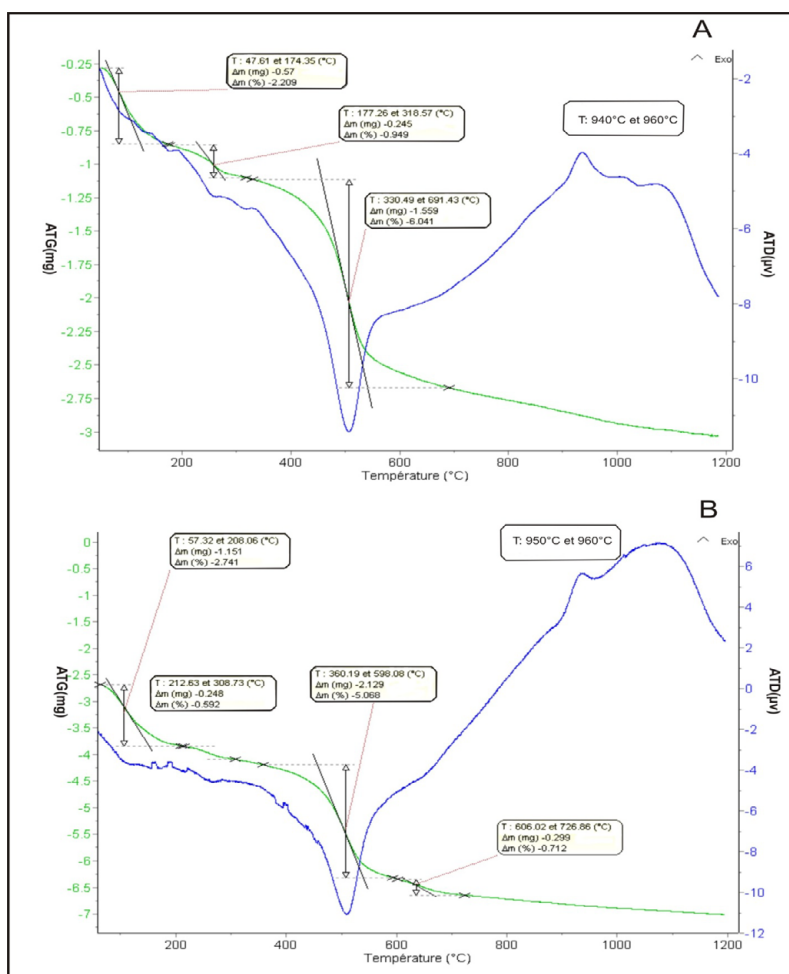


Figure 3: DTA and TGA thermograms of clays mixtures BM (A) and MK (B).

Mixtures	Whole rock					Clay fraction		
	Quartz	Calcite	Feldspars	Phyllosilicates	Hematite	Kaolinite	Illite	Smectite
BM	35	6	tr	58	0	48	6	46
MK	51	2	6	39	2	42	20	38

Table 2: Mineralogical composition of BM and MK the mixtures (Wt.%).

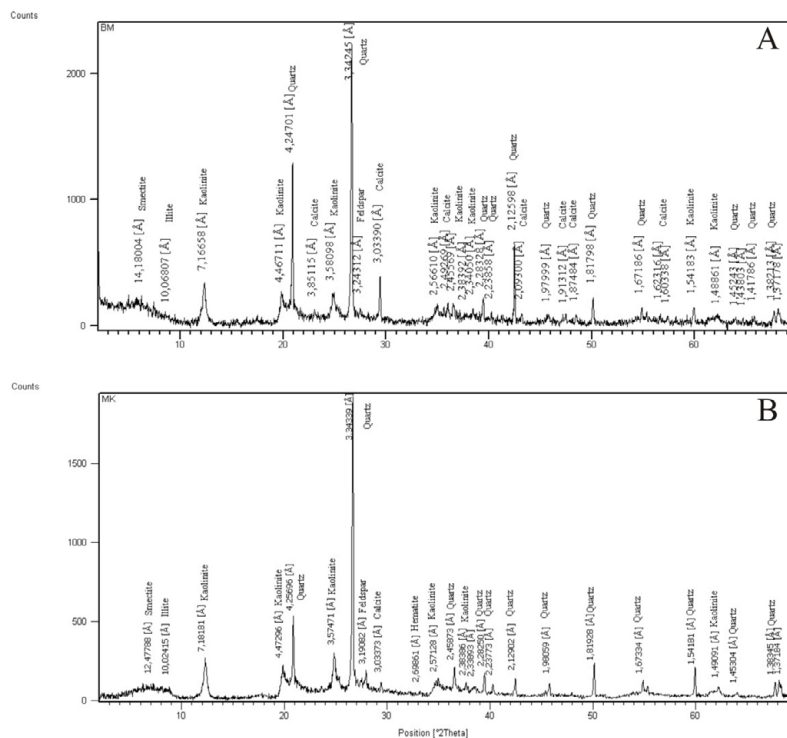


Figure 4: XRD pattern of clay powder for BM (A) and MK (B).

Major elements	BM	MK
SiO <sub>2</sub>	54.17	57.87
Al <sub>2</sub> O <sub>3</sub>	19.43	18.22
MgO	0.90	1.471
Fe <sub>2</sub> O <sub>3</sub>	9.5	10.48
CaO	5.755	2.245
K <sub>2</sub> O	1.838	2.228
Na <sub>2</sub> O	0.17	0.14
TiO <sub>2</sub>	1.494	1.408
P <sub>2</sub> O <sub>5</sub>	0.1536	0.120
MnO	0.0177	0.022
SO <sub>3</sub>	0.4732	1.432
LOI	6.13	5.25
SiO <sub>2</sub> /Al <sub>2</sub> O <sub>3</sub>	2.78	3.17

Table 3: Chemical analyses of the major elements (%), loss on ignition (LOI) in weight %, of BM and MK mixtures. (Wt.%).

1098, 1045, 798, 471 cm<sup>-1</sup>. As conclusion, the IR spectra of BM and MK clay characterise a natural mixture composed by kaolinite, illite and smectite minerals.

### Chemical characterization

**Major elements and trace elements analyses:** Table 3 shows the

results of the major elements and trace elements analyses of the (BM) and (MK) mixtures. The SiO<sub>2</sub> contents are 54.17% and 57.87% for BM and MK samples respectively. Concerning the Al<sub>2</sub>O<sub>3</sub>, we reported 19.43% and 18.22% for BM and MK mixtures respectively. The contents of alkalis (K<sub>2</sub>O + TiO<sub>2</sub>) are moderately high for both mixtures (3.332% for BM, 3.628% for MK). The content of Fe<sub>2</sub>O<sub>3</sub> is relatively high for both mixtures (9.5% for BM and 10.48% for MK) which is assigned to the presence of hematite. This value is acceptable for the use in the ceramics industry. The significant amount of CaO is assigned to the presence of carbonates. SO<sub>3</sub> values are insignificant, and are linked to the Pb-Zn sulphide reported in Kef Lasfar mine. Chemical results of trace elements show that MK samples are enriched in, Ni, Co, Ce, Ta, Pb, Sb, whereas, BM samples reveals higher contents in Cu, La, Pr, Br and Au (Table 4).

**Cation exchange capacity and specific surface:** The values of cation exchange capacity (CEC) of clays BM and MK are 52 méq/100 g for BM and 47 méq/100 g for MK respectively. The low values are due to the abundance of kaolinite and to the presence of non-clay minerals. The specific surface area (BET) of the studied clays is low: 77.77 m<sup>2</sup>/g for BM and 59.81 m<sup>2</sup>/g for MK. These values confirm that the studied clays are a mixture (semi-kaolin-semi-illito-smectic).

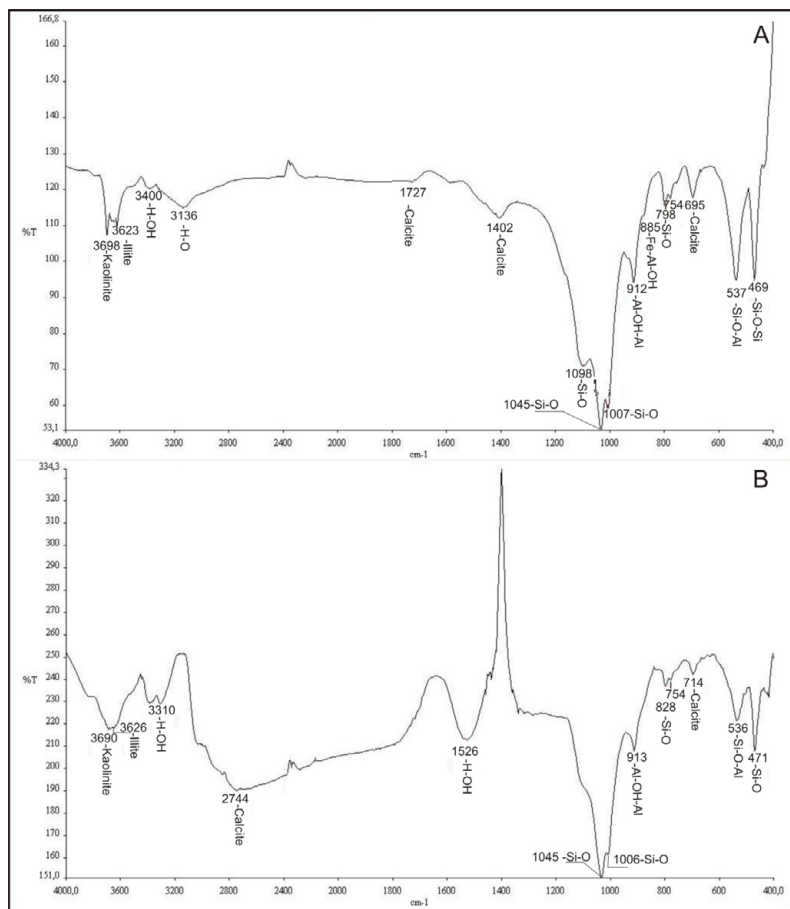


Figure 5: FTIR spectra of clays mixtures BM (A) and MK (B).

## Thermal behaviours

**Thermal Analysis:** The DTA-TGA curves of the prepared mixtures (Figures 6 and 7) show: (i) a significant endothermic peak at around 100°C, resulting from the removal of adsorbed and interlayer water of the clay minerals [24]. It represents a 2.209% (for BM) and 2.741% (for MK), weight loss of water moisture and hygroscopic water; (ii) an endothermic peak around 300°C is assigned to the combustion of organic material; (iii) an endothermic peak at 540°C attributed to the dehydroxylation of kaolinite; (iv) an endothermic peaks between 606°C and 726°C with a weight loss of 0.719% corresponds to the dehydroxylation of smectite; (v) an exothermic peak at around 950°C corresponds to the reorganization of the structure of metakaolin in Mullite.

**Dilatometry:** The Thermo-dilatometric curve of MK mixture shows a slight dilation at 88.1°C followed by a low shrinkage (4.01%) observed at 144.8°C (Figure 8). Beyond this temperature, the curve becomes linear, which corresponds to an important dilatation. The firing temperature is around 1165°C with a total shrinkage of 4.53%. For BM mixture, the first dilatation is observed at 88°C followed by 2.82% of shrinkage occurred at 175.7°C and, confirming the departure of residual water (Figure 9). The hook observed between 500 and 700°C is linked to the presence of illite. The inflexion point at 707°C is originated from the quartz conversion. The final firing temperature corresponding to 4.70% of shrinkage occurred at 1164°C.

**Plasticity:** The results of the plasticity tests are given by the Atterberg limits (Table 5 and Figure 10). The values of the LL are about 49.74% for BM and 51.11% for MK. The PL values are 33.33% and 34.50% for BM and MK respectively, which are in agreement with the range of plasticity used for ceramic product manufacture defined in the literature (30-60%). The plasticity index PI was calculated based on the arithmetic difference of the plasticity limit and liquid limit. Both clays present relatively medium values of plasticity (7% < PI < 15%).

**Bigot Curves:** The Bigot curves of the clay mixtures (BM and MK) after drying shows that the proportions of moisture water, interlayer water and colloidal water are 24.66%, 17.61% and 7.05% respectively (Figure 11). The total shrinkage after drying is 5.51%. This value results from the substantial amount of sand in the clay samples.

## Industrial Tests

Concerning, the tiles manufacture, the results of technological tests in semi-industrial scales show a small drying shrinkage at around 1% for BM and 0.7 for MK (Table 6). Furthermore, the firing shrinkage is less than 2% for the two mixtures and depends to the firing temperature. The values of water absorption are greater than 10% for both mixtures, which is conforms to the French standard N.F.EN. 15 [25] (Table 7). Regarding the resistance to the inflection, which is the parameter defining the class of ceramic faience products according to the French standard N.F. EN 100 [26], we recorded at 1000°C 11.62 N/mm<sup>2</sup> for MK mixture and 8.56 N/mm<sup>2</sup> for BM mixture. Therefore, the results

Trace elements	BM	MK
As	3.979316	5.150252
Pb	< 1.94624	135.2637
W	1.58596	1.09105
Ta	2.047425	16.3794
Sb	< 3.33448	241.7498
Sn	1.969125	5.35602
Nb	102.75888	82.48672
Zr	808.41852	784.7286
Rb	236.83219	259.69244
Zn	3133.143	3052.806
Cu	92.6666	87.07465
Ni	40.07784	74.6548
Cr	255.2066	636.306
V	244.79429	235.2714
Ga	49	40.91835
Ge	<1	0.69405
Br	41	6,7
Sr	1452,72362	1462,8707
Y	77	90
Mo	< 3	< 3
Ag	<0.93096	<0.93096
Cd	< 1	< 1
Te	3	100
I	180	<30
Cs	600	540
Ba	2,9	510
La	119	1
Ce	<1	100
Pr	100	46
Nd	55	83
Hf	<9.7	57
Pt	< 2	< 2
Au	17	< 2
Hg	7	19
Th	600	60
U	7.8	7.4
Co	< 53.3528	94.3776

Table 4: Chemical analyses of the trace and rare earth elements of clay mixtures (ppm).

Mixtures	LL	PL	PI
BM1	49.74	33.33	16.41
MK1	51.11	34.50	16.61

Table 5: Atterberg limits (%).

Mixtures	Temperature (°C)	Breaking Load	Flexural strength N/mm <sup>2</sup>	Breaking force	Removing Cooking (RC %)	Linear firing shrinkage (LF %)	L.O.I (%)	Water absorption (WA%)
MK	950	256.04	6.63	217.49	1.04	1.44	9.24	14.08
	1000	312.94	11.62	271.87	1.00	1.57	9.61	13.05
BM	950	211.90	6.58	172.44	0.71	1.65	10.96	14.69
	1000	246.23	8.56	200.65	0.69	1.81	11.08	14.17

Table 6: Composition of mixtures and corresponding measured values of flexural strength, water absorption, the linear firing shrinkage, the Removing Cooking and the L.O.I. for ceramic faience.

of semi-industrial technological tests for the tiles are similar. For the ceramic brick fabrication, we consider only one mixture combining BM and MK clays. The drying shrinkage values are around 7.70% and the removing cooking values are 0.44% at 800°C. It becomes 1.8% at 850°C and evolves to 3.89% at 900°C. The water absorption reduces from 14.70 to 7.78% when the temperature shifts from 800°C to 900°C (Table 7).

## Discussion

In order to assess the potentiality of Mjez el Beb clays in the ceramic industry, their mineralogy, chemistry composition, thermal behaviours and technological properties were determined. The results showed the predominance of the fine fraction composed basically with kaolinite, smectite and illite which are confirmed by the infrared spectroscopy. The confectioned items made of these clays have a red to dark colour arising from the high concentration of iron oxides content. This later, lead to a good fluxing properties and affect the mechanical strength of the ceramic products [27,28]. In addition, Fe<sub>2</sub>O<sub>3</sub> with alkaline elements favour the formation of vitreous phase and lead to the densification of these fine materials and therefore could affect their fluxing and the firing temperatures [29]. The weight loss on ignition occurring after sintering lead to the development of the porosity, and has an effect on the resistance to the inflection during the thermally treatment. Beside, this clays are enriched in some trace elements such as Zn Sr, Cr, Th, Cs, Nb, V, Zr and Y. Zn Sr, Cr, Th which could be mobilized by the mineralizing fluids of the Kef Lasfer mine. These elements have an important role in the improvement of the mechanical resistance of the ceramic products. Previous studies showed that the Cs, Nb and V enhance the melting point as well as the mechanical strength. Whereas, the Zr present as oxide (zirconia), or silicate (zircon) could improve the ceramic materials quality. Beside, Y could be used as a sintering additive [30]. During the thermal treatment, various reactions occur principally dehydration, dehydroxylation and structural reorganization and neoformation phases.

## Structural transformations

During firing treatment, clay minerals are transformed into new minerals dehydrated. At 850°C, kaolinite is transformed into amorphous phase: metakaolinite (Al<sub>2</sub>Si<sub>2</sub>O<sub>7</sub>) by the removal of the hydroxyl groups of the silicate lattice according to the following reaction: Al<sub>2</sub>Si<sub>2</sub>O<sub>5</sub>(OH)<sub>4</sub> → Al<sub>2</sub>Si<sub>2</sub>O<sub>7</sub> + 2H<sub>2</sub>O.

Between 850°C and 950°C, the CaCO<sub>3</sub> decomposes to CaO accompanied by disengagement of CO<sub>2</sub> outside the structure of fired bodies; this phenomenon creates a porous structure [29]. The CaO reacts with the metakaolinite at increasing temperature, leading to the

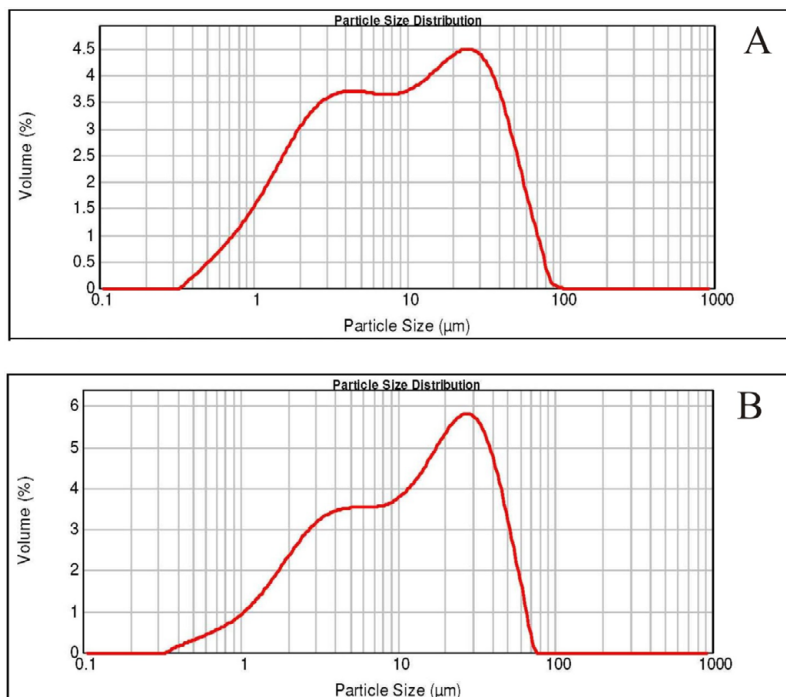


Figure 6: Granulometric analyses of clays mixtures BM (A) and MK (B).

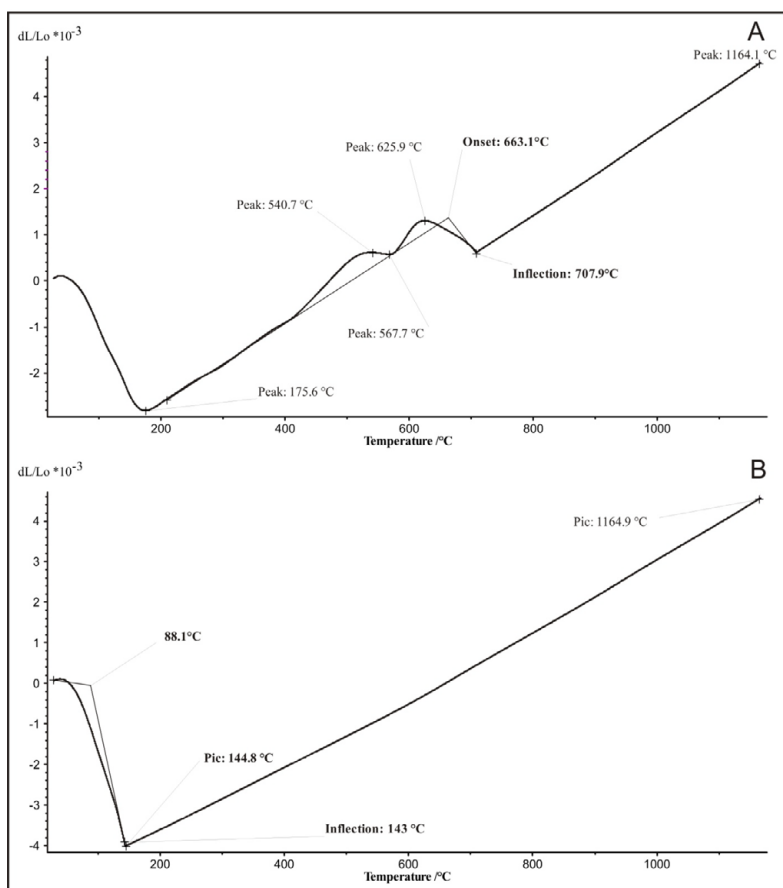


Figure 7: Dilatometric curve of clays mixtures BM (A) and MK (B).

	Linear firing shrinkage (LF %)	Firing temperature (°C)	Removing Cooking (%)	L.O.I (%)	Water Absorption (WA%)
(BM + MK) Mixture	7,70	800	0.44	9.55	14.70
		850	1.8	9.62	11.31
		900	3.89	9.90	7.78

Table 7: Technological properties of the prepared ceramic bricks.

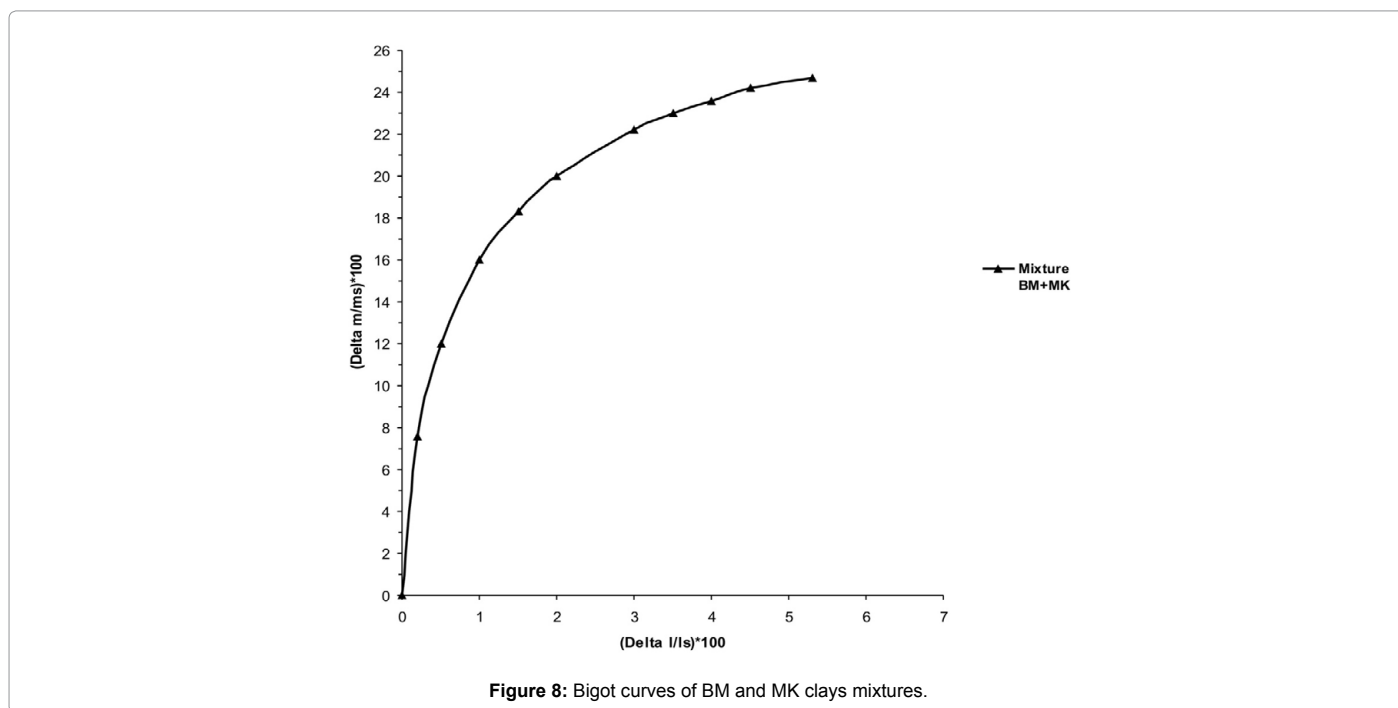


Figure 8: Bigot curves of BM and MK clays mixtures.

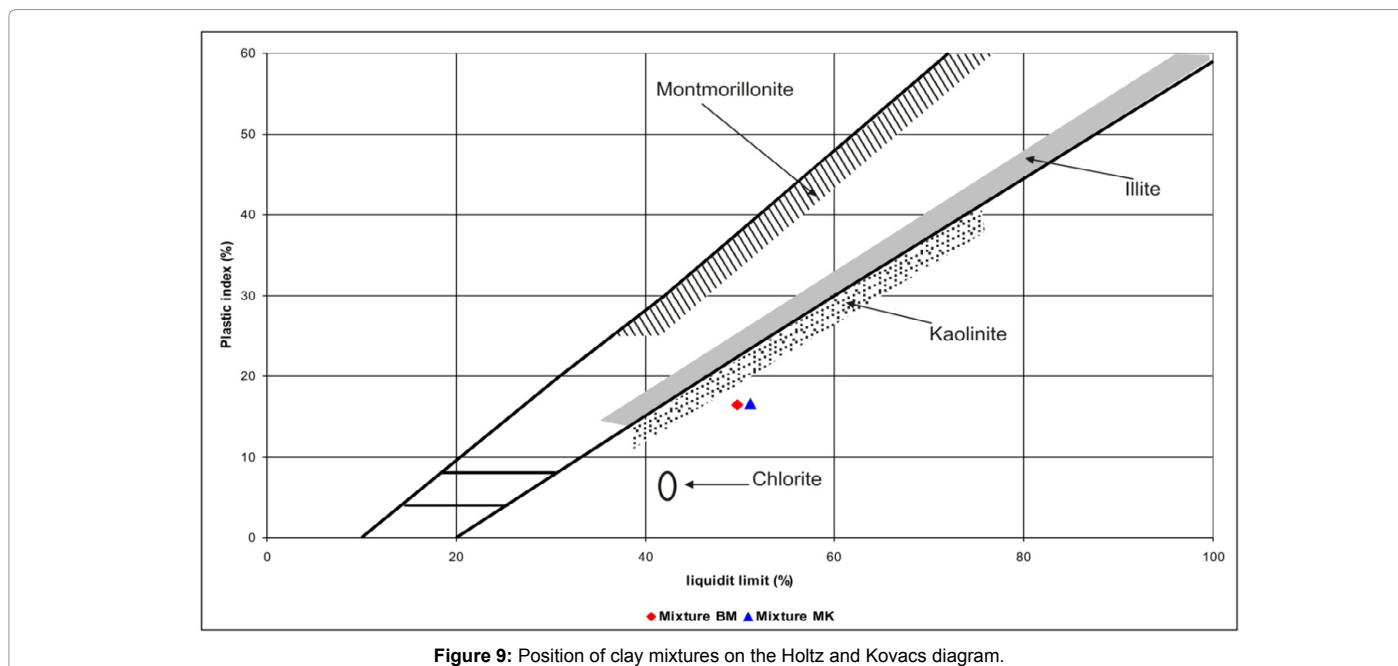
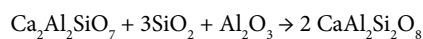
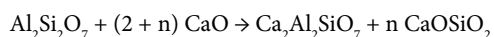


Figure 9: Position of clay mixtures on the Holtz and Kovacs diagram.

formation of the gehlenite which evolves to anorthite [31,32] (Figures 12 and 13) according to the following reaction:



In general, we cannot exclude the formation of anorthite from the metakaolinite according to the reaction:



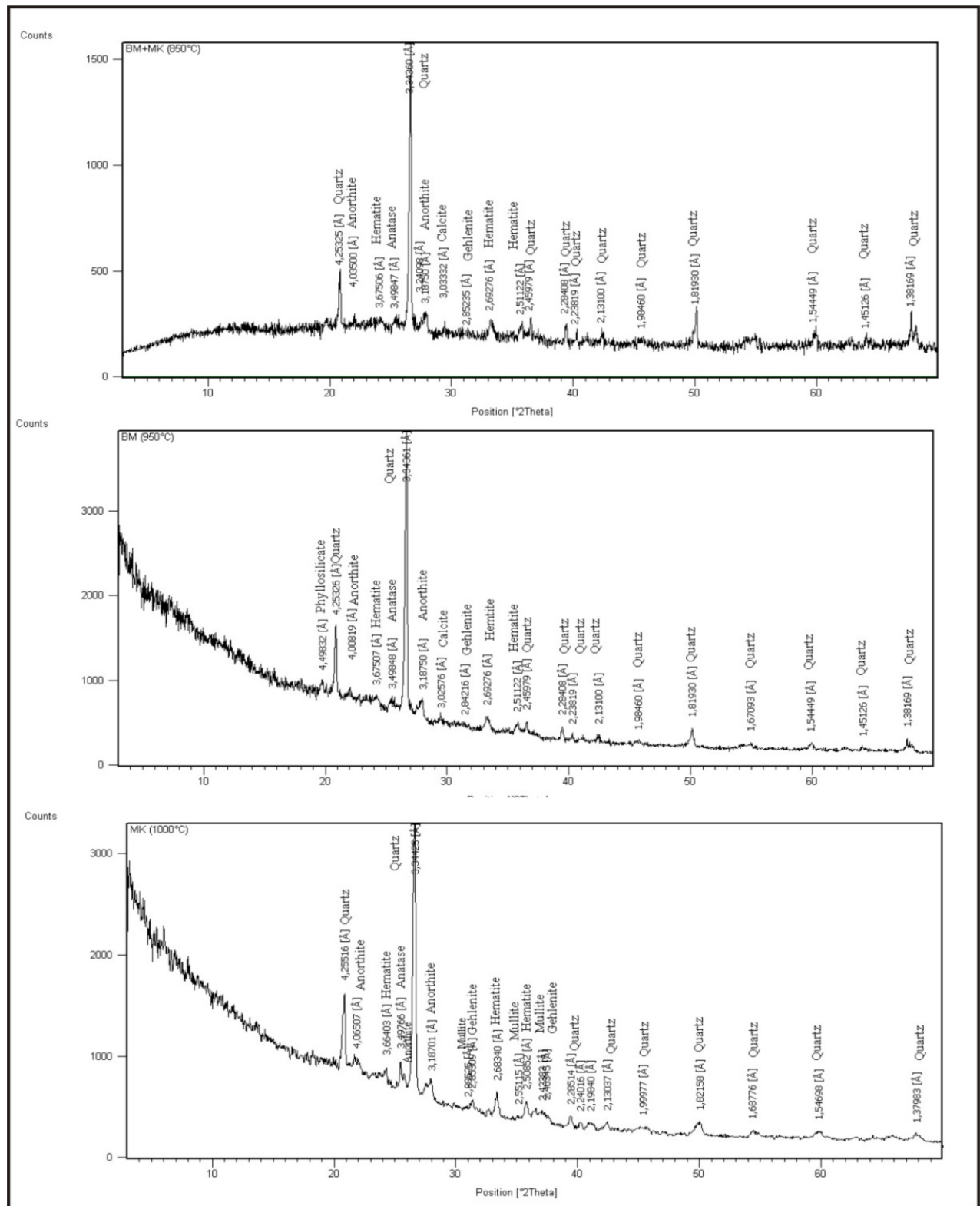


Figure 10: X-ray diffraction patterns for the mixed clays sintered at 850°C, 900°C and 1000°C.

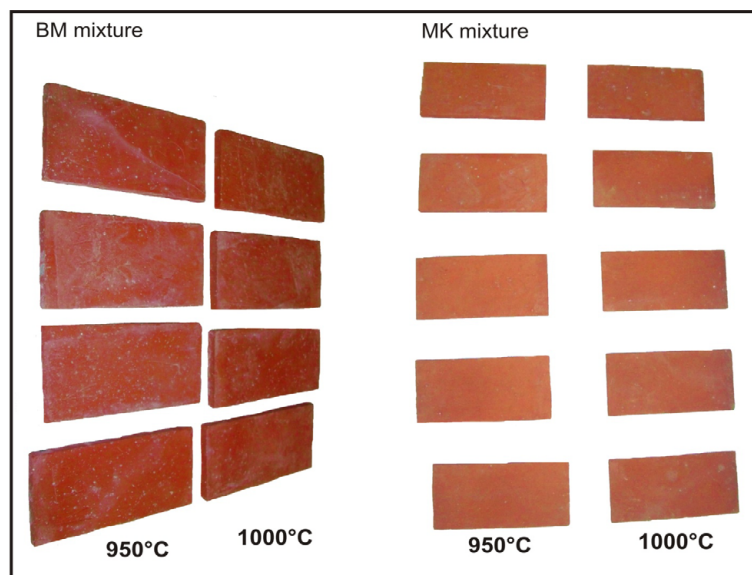


Figure 11: Ceramic faïences manufactured from clays mixtures BM and clays mixtures MK.

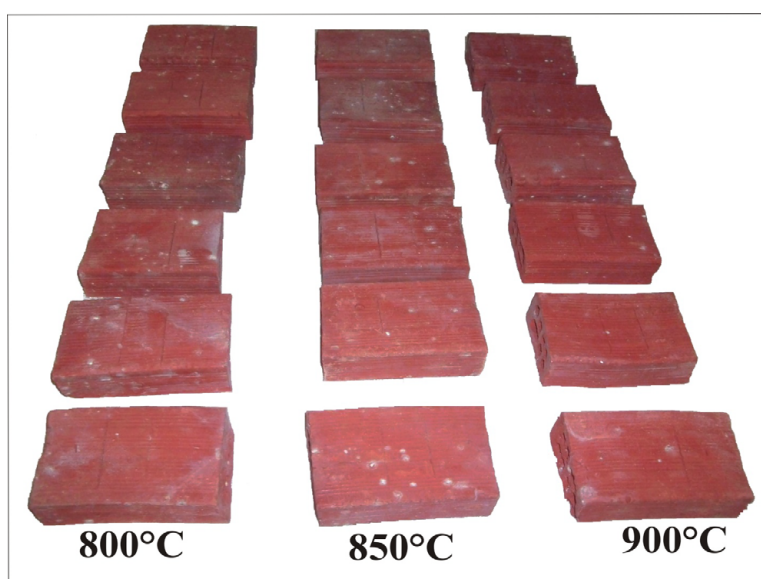
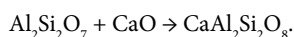


Figure 12: Ceramic bricks manufactured from clays mixtures (BM +MK).



Above 900°C, a segregated spinel-type phase ( $\gamma\text{-Al}_2\text{O}_3$ ) recrystallizes [33], and evolves to mullite when the temperature increase above 1000°C. The industrial tests carried out on the fired products reveal a low withdrawal, which is linked to the removal of the water. This latter is responsible of the tightening of the particles and the decrease of the liquid surface and capillarity tension. Concerning the mechanical resistance to the inflexion, the medium value observed is related to the medium plasticity of the Cretaceous clays. Previous studies showed that the flexural strength could be linked to the presence of silica minerals [34]. It was also shown, that the mechanical resistance to the inflexion increases with vitrification. Indeed, when vitrification is completed, the pores join together to form large pores causing the

macroscopic deformation on the ceramic materials [35-40].

## Conclusion

In conclusion, the mineralogical and geochemical characterizations of the Cretaceous clay of Mjez El Beb revealed a good quality of raw material composed mainly of kaolinite and illite and enriched with  $\text{Al}_2\text{O}_3$  and  $\text{SiO}_2$ . These oxides have a decisive influence on the refractoriness and strength of the final product. Besides that, the  $\text{Fe}_2\text{O}_3$ , alkali and alkaline earth elements, present in the clays, lead to the rapid vitrification and fusion during firing. In addition, the high proportions of finer particles favour the vitrification due to the good compaction during moulding, which positively influences on the resistance of fired materials. During firing, several mineralogical transformations of the

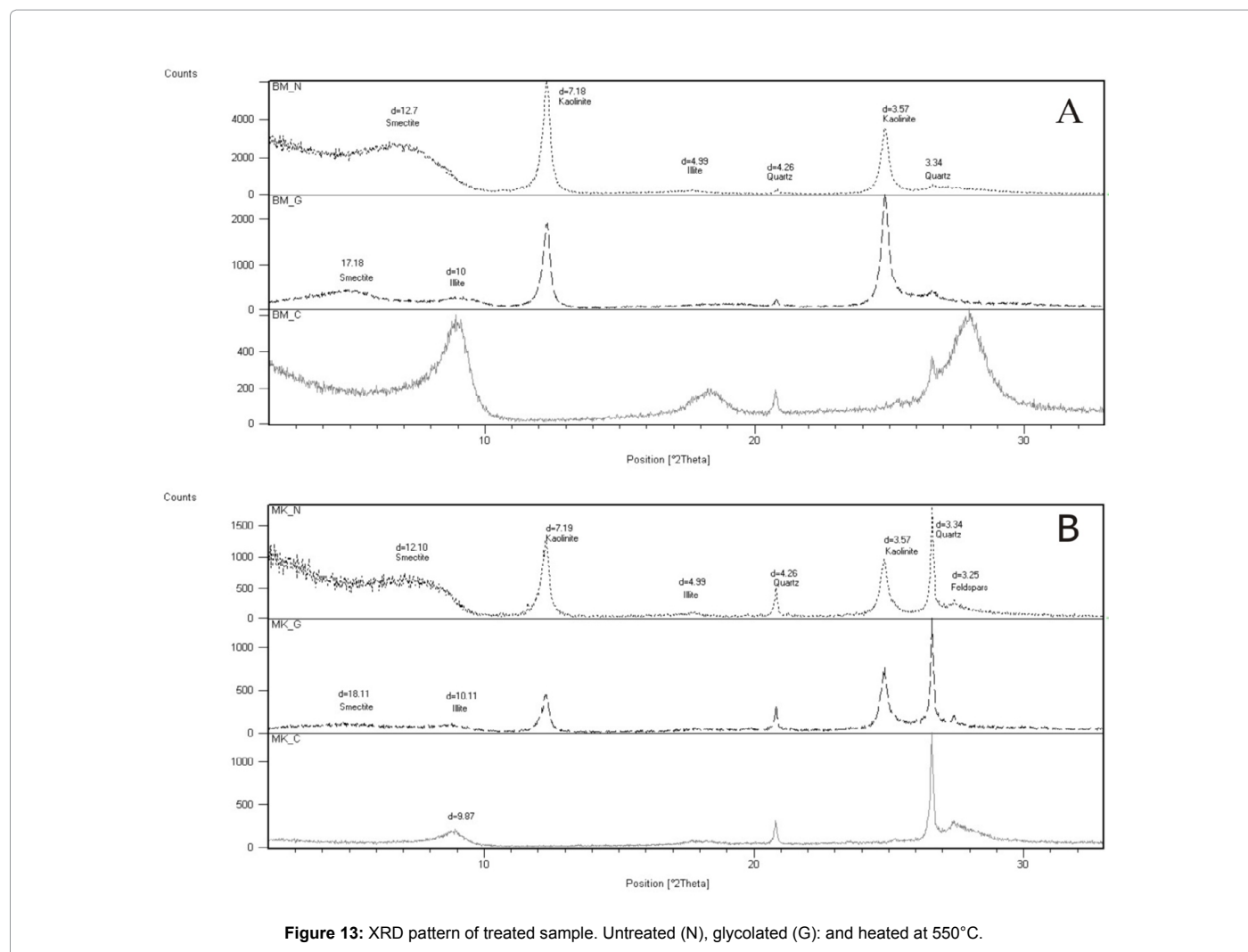


Figure 13: XRD pattern of treated sample. Untreated (N), glycolated (G): and heated at 550°C.

minerals initially present in clay powder occur [41-43]. The new phases represented mainly by metakaolinite, gehlenite, anorthite, spinel-type phase ( $\gamma\text{-Al}_2\text{O}_3$ ) and mullite enhance the process of sintering of ceramic matrix. Therefore, the mineralogical and chemical compositions allowed us to choose the suitable semi industrial manufacturing applications [44-46]. For this, we recommend to use BM and MK clay-mixture in the ceramic earthen ware, and to mix BM and MK for the bricks fabrication. The quality of the ceramic product could be verified by examining the firing shrinkage, the firing line narrowing, the ignition loss, the porosity, the plasticity and the flexural strength.

#### Acknowledgment

This work was carried out in the University of Sciences, Tunis, Tunisia, Centre Technique des Matériaux de Construction, de la Céramique et du Verre "C.T.M.C.C.V", Centre de Recherches et des Technologies des Eaux Technopole de Borj-Cédria. We thank Mrs Bargaoui Latifa for her helpful contribution of thermal analyses.

#### References

- Grim RS (1960) Application of clay mineralogy.
- Hammami M (1999) Ectonics, Holocene and implementation mineralization in the diapirs zone (Tunisie septentrional), Thesis, University Tunis, Tunisia, (183pp).
- Bolze J (1954) Ascension and pierced through diapirs in the mountains of

Cretaceous Téboursouk (Tunisie septentrionale). *CR Soc géol France*: 139-141.

- Perthuisot V (1978) Dynamic and petrogenesis of Triassic extrusions in northern Tunisia. Thesis es Ecole Normale Supérieure Sciences, Paris. (312 pp).
- Rouvier H, Perthuisot V, Mansouri A (1985) Deposits and salt bearing diapirs in southern Europe and North Africa. *Econ Geol* 80: 666-687.
- Benassi R, Jallouli C, Hammami M, Turki MM (2006) The structure of Jebel El Mourra, Tunisia: A diapiric structure causing a positive gravity anomaly. *Terra Nova* 18: 432-439.
- Bejaoui J, Bouhlef S, Cardellach E, Canals À, Perona J, et al. (2013) Mineralization and fluid inclusion studies of the Aptian carbonate-hosted Pb-Zn-Ba ore deposits at Jebel Hamra, Central Tunisia. *J Geochem Explor* 128: 136-146.
- Marie J, Trouve P, Desforges G, et Dufaure P (1984) New elements of the Cretaceous paleogeography of Tunisia. *Notes et Mém., CFP* 19: 7-37.
- Orgeval JJ (1994) Metal concentration Peridiapiric: example of the Bougrine deposit (Tunisia Atlas). In: Fontboté L, Boni M (eds) *Sediment-hosted Zn-Pb right*. Springer, Heidelberg, Applied to Mineral Deposits, Special Publication 10: 354-389.
- Salaj J (1978) The geology of the Pelagian block; The eastern Tunisian platform. In: Nairn AEM, Kanes WH, Stehli FG (eds.) *The ocean basins and margins; The western Mediterranean, v.4B*: New York, Plenum Press: 361-416.
- Maamouri AL, Zaghbib-Turki D, Matmati MF, Chikhaoui MI, Salaj J (1994) The Bahloul formation centro-northern Tunisia: New lateral variation dating and new

- interpretation in terms of sequence stratigraphy. *J African Earth Sci* 18: 37-50.
12. Van Hinte JEA (1976) Cretaceous time scale, *Amer Ass Petrol Geol Bull* 60: 498-516.
  13. Meseguer S, Sanfeliu T, Jordan MM (2009)b. Classification and statistical analysis of mine spoils chemical composition from Oliete Basin (Teruel. NE Spain). *Environ Geol* 56: 1461-1466.
  14. ISO 10545-4 (2014) Ceramic tiles: Determination of flexural strength and fracture strength.
  15. Farmer VC (1974) The layer silicates in the infrared spectra of minerals. pp 331-365.
  16. Van der Marel HW, Beutelspacher H (1976) *Atlas of Infrared Spectroscopy of Clay Minerals and their Admixtures*: Elsevier, Amsterdam: pp 396.
  17. Kodama Y (1985) Optical solitons in a monomode fiber. *J Statistical Physics* 39: 597-614.
  18. Balan E, Saitta AM, Mauri F, Calas G (2001c) First-principles modeling of the infra-red spectrum of kaolinite. *Am Mineralogist* 86: 1321-1330.
  19. Benco L, Tunega D, Hafner J, Lischka H (2001)b. Orientation of OH groups in kaolinite and dickite: Ab initio molecular dynamics study. *American Mineralogist* 86: 1057-1065.
  20. Van der Marel H, Krohmer W (1969) OH stretching vibrations in kaolinite and related minerals. *Contributions to Mineralogy and Petrology* 22: 73-82.
  21. Farmer VC (2000) Transverse and longitudinal crystal modes associated with OH stretching vibrations in single crystals of kaolinite and dickite. *Spectrochimica Acta. Part A: Molecular and Biomolecular Spectroscopy* 56: 927-930.
  22. Borchardt GA (1977) Montmorillonite and other smectite minerals: In *Minerals in Soil Environments*, Dixon JB, Weed SB (eds.), Soil Sci Soc Amer, Madison, Wisconsin: 293-330.
  23. Mendelovio E, Yariv S, Villalba R (1979) Iron-bearing kaolinite in Venezuelan laterites. I. Infrared spectroscopy and chemical dissolution evidence. *Clay Miner* 14: 323-331.
  24. Baran B, Ertürk T, Sarikaya Y, Alemdaroğlu T (2001) Workability test method for metals applied to examine a workability measure (plastic limit) for clays. *Applied Clay Sci* 20: 53-63.
  25. Afnor EN 159 (1991) Ceramic tiles, Determination of the water absorption 61p.
  26. Afnor EN 99 (1982) Ceramic tiles, Determination of the water absorption 6p.
  27. Anderson CR, Siegel DA, Kudela RM, Brzezinski MA (2009) Empirical models of toxigenic *Pseudo-nitzschia* blooms: Potential use as a remote detection tool in the Santa Barbara Channel. *Harmful Algae* 8: 478-492.
  28. Samara M, Lafhaj Z, Chapiseau C (2009) Valorisation of stabilized river sediments in fired clay bricks: Factory scale experiment. *J Hazardous Mater* 163: 701-710.
  29. Darweesh HHM (2001) Utilization of cement kiln by-pass dust waste as a source of CaO in ceramic industry. *Silicates Industrials* 66: 47-52.
  30. Habashi F (2001) Historical Introduction to Refractory Metals, *Mineral Processing and Extractive Metallurgy Revue* 22: 25-53.
  31. Jouenne CA (1984) *Ceramics trafficking Minerals and Materials*, Editions Septima Paris.
  32. Traore K (2003) Low temperature sintering of a kaolinitic clay in Burkina Faso. *Transformations thermiques et réorganisations structurales*. Thèse de Doctorat pp: 140.
  33. Colegrave EB, Rigby GB (1952) The decomposition of kaolinite by heat: *Trans. Brit Ceram Soc* 51: 355-367.
  34. Baccour H, Medhioub M, Jamoussi F, Mhiri T, Daoud A (2008) Mineralogical evaluation and industrial applications of the Triassic clay deposits, Southern Tunisia. *Mater Charact* 59: 1613-1622.
  35. Anderson M, Elliott M, Hickson C (2002) Factory scale trials using combined mixtures of three byproduct wastes (including incinerated sewage sludge ash) in clay building bricks. *J Chemical Technol Biotechnol* 77: 345-351.
  36. Chang LLY (2002) *Industrial Mineralogy: Materials, Processes and Uses*. Upper Saddle River, NJ: Prentice-Hall.
  37. Dondi M, Ecolani G, Guarini G, Marsigli M, Mingazzini CV (1999) Major deposit of brick clays in Italy: part 2. Technological properties and uses. *Tile Brick Int* 15: 360-370.
  38. Franco F, Cecilia JA, Pérez-Maqueda LA, Pérez-Rodríguez JL, Gomes CSF (2007) Particle-size reduction of dickite by ultrasound treatments: effect on the structure, shape and particle-size distribution. *Applied Clay Science* 35: 119-127.
  39. Gadsen JA (1975) *Infrared Spectra of Minerals and Related Inorganic Compounds*. Butterworths, London.
  40. Gunasekaran S, Anbalagan G (2007) Spectroscopic characterization of natural calcite minerals. *Spectrochimica Acta (Part A)* 68: 656-664.
  41. Jamoussi F, Bédir M, Boukari N, Kharbachi S, Zargouni F, et al. (2003) Clay mineralogical distribution and tectono-eustatic control in the Tunisian margin basins. *CR Acad Sci* 335: 175-183.
  42. LCPC (1987) Atterberg limits, liquid limit, plastic limit, test method LPC, n°19, publication L. C. P. C. 26.
  43. Massrouhi A (2006) The salt-bearing devices of Mateur region Tebourba and Bab El Mjez (Tunisie Nord). Thesis University Tunis, Tunisie pp: 260pp.
  44. Rouvier H (1977) Geology of the extreme north of Tunisia: paleogeography and tectonic superimposed at the eastern end of the northern Maghreb channel. Thèse ès Sciences, Univ. Paris VI pp: 634.
  45. Sdiri A, Higashi T, Hatta T, Jamoussi F, Tase N (2010) Mineralogical and spectroscopic characterization and potential environmental use of limestone from the Abiod formation, Tunisia. *Environ Earth Sci* 61: 1275-1287.
  46. Van OH (1963) *An Introduction to Clay Colloid Chemistry*: Interscience, New York: 94-95.